Instantaneous Phase Maps in Cardiac Arrhythmias: Comparison Between Sinusoidal Recomposition and Hilbert Transform

Giovanni Viriato Critelli[1], Jimena Siles Paredes[1], Tainan Cerqueira Neves[1], Saleem Ullah[1], Angélica Drielly Quadros[1], José Gomes Junior[1], João Salinet[1]

[1]HEartLab, Federal University of ABC, São Bernardo do Campo, Brazil

Abstract

This study evaluated the reconstruction of the instantaneous phase of cardiac signals during atrial fibrillation (AF), ventricular fibrillation (VF), and ventricular tachycardia (VT) using optical recordings from Langendorff-perfused rabbit hearts provided by HeartLab (UFABC). The phase was obtained by direct application of the Hilbert Transform (HT) and compared with the Sinusoidal Recomposition (SR) method, which reconstructs signals as a sum of sinusoids with period equal to the dominant frequency. Phase maps were generated to identify singularity points (SPs), clusters, and filaments. Visually, both methods produced similar patterns, but SR maps showed sharper contours, while HT Direct yielded smoother transitions. Similarity analysis confirmed high agreement, although quantitative differences were evident. The HT Direct consistently detected higher numbers of SPs, clusters, and filaments, possibly reflecting overestimation. In contrast, SR reduced detections and acted as a filtering step, particularly in VF. SR also increased median filament size with higher variability, whereas HT produced shorter and more consistent filaments. Overall, SR is a promising alternative to the HT Direct approach for analyzing reentry patterns in noisy or non-sinusoidal signals.

1. Introduction

Cardiac arrhythmias represent disturbances in the electrical conduction of the heart and can range from benign conditions to potentially fatal ones, such as ventricular fibrillation (VF) and ventricular tachycardia (VT) [1]. Atrial fibrillation (AF), the most common arrhythmia in clinical practice, is associated with a high risk of thromboembolic events and mortality, especially in elderly populations. Identifying and understanding the electrophysiological mechanisms underlying these arrhythmias is essential for proper diagnosis and treatment.

Treatment of arrhythmias can involve the use of antiarrhythmic drugs or catheter ablation procedures; the latter being considered more effective for certain types of AF. Ablation requires precise mapping of electrical activation to locate ectopic foci and reentry pathways. Electrical mapping with electrograms recorded directly from the epicardium is a widely used technique, but is limited by its invasive nature, reduced spatial coverage and limited resolution.

As an alternative, optical mapping has been used in experimental models, offering high temporal and spatial resolution in the observation of cardiac electrical activity [2]. However, its clinical application is still restricted, mainly due to the use of potentially toxic fluorescent dyes.

A complementary approach to conventional mapping is the construction of phase maps, which allows the identification of reentry patterns in complex arrhythmias. To do this, it is necessary to extract the instantaneous phase of cardiac signals. The technique traditionally used is to apply the Hilbert Transform (HT) directly to the signals, which is effective for signals with quasi-harmonic behavior. In contrast, the sinusoidal recomposition (SR) method, proposed by Kuklik et al. (2015) [3], transforms the cardiac signals into a sum of sinusoids, enabling a more robust estimate of the instantaneous phase.

In this work, we propose the application of the SR method to reconstruct the instantaneous phase in optical signals obtained from rabbit hearts submitted to Langendorff-type perfusion and induction of AF, VF and VT arrhythmias. The phase obtained by SR was compared with the phase estimated by direct application of HT, with a focus on generating and performing a quantitative analysis of singularity points (SPs), clusters, and filaments.

The data was provided by the HEartLab group (UFABC), with simultaneous optical and electrical recordings. It is believed that this approach can offer improvements in the analysis of the dynamics of complex arrhythmias, contributing to the development of more precise mapping and ablation strategies.

2. Methods

2.1. Data Acquisition

Cardiac signals obtained from rabbit hearts perfused by the Langendorff system were analyzed in trials carried out by the HEartLab research group at UFABC, with approval from the Ethics Committee (protocols no. 3947230519 and 5612190822). Full details are described in [4]. The

electrical recordings were obtained by three unipolar contact microelectrodes (MEAs), with 16 electrodes arranged in a 4×4 matrix, positioned in the right atrium, ventricle and left atrium. The optical signals were captured by three high-speed cameras (500 fps, 1600×1000 px, Emergent Technologies), arranged at 120° around the heart. Recordings were analyzed in sinus rhythm and under induced arrhythmias: AF, VF and VT.

2.2. Signal Pre-Processing

A binning factor of 8 was applied to the optical data prior to filtering, and the signals underwent baseline correction with a high-pass filter (Butterworth, 0.5 Hz), followed by smoothing with a spatio-temporal Gaussian filter (5×5 spatial kernel, 1×7 temporal kernel) [4].

2.3. Instantaneous Phase Calculation

The instantaneous phase was obtained using two approaches: (i) application of the HT directly to the original signals, and (ii) application of the SR method. In the SR approach, the signal is transformed using a sum of sinusoids with a period equal to the mean cycle length. The phase is then calculated on the reconstructed signal. To align the phase discontinuity with the depolarization events, an adaptation was made to the phase calculation to ensure that the inversion points coincided with these events [3]. The phase definition used for optical signals is shown in (1).

The mean cycle length required for the SR was estimated from the Dominant Frequency (DF), defined as the frequency with the highest amplitude within a characteristic range for each phenomenon, calculated over the central window of the signal. For arrhythmic signals, the DF was searched within 3–12 Hz, a range that encompasses physiologically plausible cycle lengths for AF, VF, and VT while excluding low-frequency drift and high-frequency noise.

$$\phi = \tan^{-1}\left(\frac{-u(t)}{H(u(t))}\right) \quad (1)$$

2.4. Phase Maps and Singularity Point Detection

Phase maps were generated using both the traditional approach and the SR method for comparison. Each camera produced a data volume of 125 × 200 × 2500, and the instantaneous phase was computed for each voxel before and after SR application. To visualize the spatiotemporal evolution of the phase, videos of 2,500 frames were generated at 30 fps, downsampled from the original 500 fps acquisition, with colors representing phase values between $-\pi$ and π.

SPs were initially identified manually in each frame by observing regions of rotational phase. Subsequently, an algorithm was applied to detect SPs within a region of interest (ROI). First, edges were extracted using the Canny detector, and endpoints identified with the MATLAB *bwmorph* function were considered candidate SP. For each endpoint, the phase progression was evaluated in three concentric rings (eight neighbors each). A valid SP required at least two rings to exhibit an ordered phase progression covering almost $0.6 \cdot 2\pi$ (≈3.8 rad), with no phase leaps greater than $0.4 \cdot 2\pi$ (≈2.5 rad). Finally, the rotation direction was determined, and the SPs were plotted on the phase maps.

2.5. Phase Maps Similarity, Clusters and Filaments

To compare the HT Direct and SR phase maps, similarity was quantified as the mean angular difference between them. For each pixel, the angular difference was calculated, and the average across all pixels was then obtained. This procedure was repeated for all 2,500 frames, and a final mean difference was computed.

Clusters with concentration of SPs were obtained using connected component analysis with an 8-neighbor connectivity in the heatmaps, and the number of clusters was quantified. Heatmaps were defined as the histogram of the SPs.

A filament was defined as the connection of the SPs along subsequent frames. Two SPs were considered connected if their Euclidean distance was ≤ 10 pixels, and a valid filament must contain at least 5 consecutively connected SPs.

3. Results and Discussion

3.1. Phase Maps Similarity

Across the three rhythms and optical fields, the phase maps obtained with both methods were highly similar, confirming overall agreement (Figure 1).

When visually comparing the phase maps (Figure 2), it can be seen that both produce similar patterns. However, the maps generated with the SR method show more defined segmentations between colors, highlighting individual pixels, while the maps obtained by the traditional method show a more continuous distribution of colors, resulting in a smoother and more fluid visual representation. This difference suggests that the HT Direct smooths out phase transitions, while SR better preserves contours between regions with different phase values.

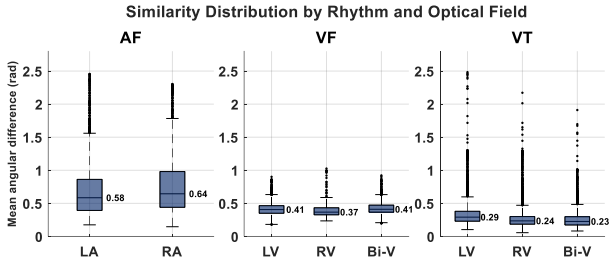

Figure 1. Similarity Distribution by Rhythm and Optical Field compared between HT Direct and SR phase maps, the similarity was quantified as the mean angular difference.

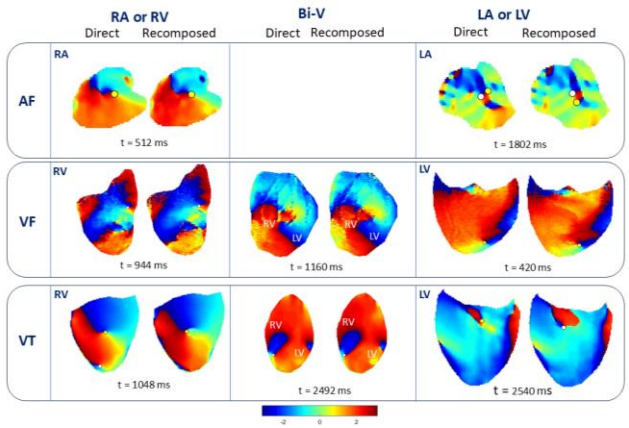

Figure 2. Phase maps organized by rhythm and cardiac region. HT Direct maps are shown on the left and SR maps on the right; SPs are marked as yellow (counterclockwise) or white (clockwise) circles.

3.2. Singularity Points

The number of SPs detected is summarized in Figure 3, grouped by experiment and optical field for both HT Direct and SR approaches. Overall, the HT Direct consistently produced higher SP counts across all conditions. In VF, the SR method substantially reduced the number of detected SPs, while in VT the reduction was less pronounced but still evident. This trend suggests that the SR method attenuates spurious detections, particularly in more disorganized rhythms such as VF.

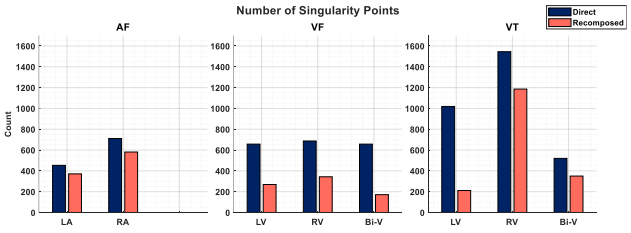

Figure 3. Number of SPs detected for AF, VF, and VT across the optical field, comparing HT Direct and SR phase maps.

3.3. Clusters

The number of SP clusters is shown in Figure 4. Across all experiments, the HT Direct consistently produced a greater number of clusters compared to the SR approach (Figure 5). In AF, clusters were detected in LA and RA with the HT Direct (9 and 8, respectively), but were markedly reduced with the SR (6 and 2, respectively). In VF, the reduction was even more pronounced: HT Direct detection yielded 10–19 clusters, whereas the SR resulted in only 1–3 clusters per camera. For VT, the HT Direct produced 10–12 clusters per camera, while the SR reduced the counts but still preserved a moderate number of clusters (5–8).

Overall, these results suggest that the SR not only decreases the number of SPs but also reduces their aggregation into clusters, particularly in VF, which is consistent with the hypothesis that SR suppresses spurious or unstable detections.

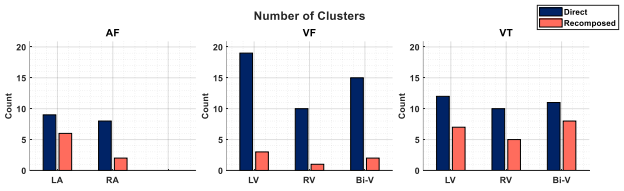

Figure 4. Number of SPs clusters detected for AF, VF, and VT across the optical field, comparing HT Direct and SR phase maps.

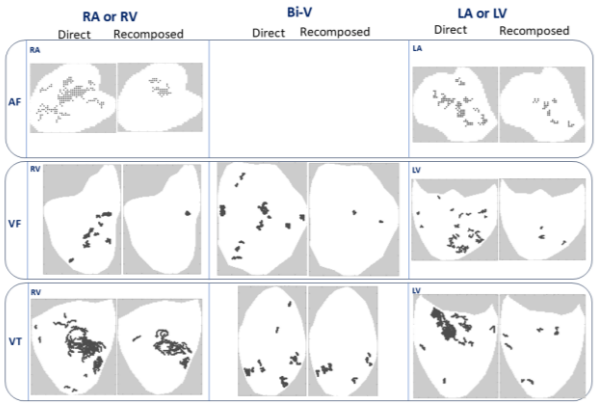

Figure 5. Clusters maps organized by rhythm and optical field. HT Direct maps are shown on the left and SR maps on the right;

3.4. Filaments

The number of filaments identified in each condition is presented in Figure 6. In AF, the HT Direct yielded 16 and 40 filaments in LA and RA; the SR reduced the counts in RA (26) but slightly increased them in LA (22). In VF, HT Direct detection produced 13–26 filaments, whereas the SR consistently reduced these values (9–13). For VT, the

HT Direct resulted in the highest filament counts overall (33–58), while the SR substantially reduced them in LV (7) and Bi-V (16), but preserved a comparable number in RV (52).

Figure 7 shows the distribution of filament sizes. Overall, the SR increased the median filament size, but with higher variability across some regions. Conversely, the HT Direct produced smaller filaments with less variability. This suggests that SR favors longer but more variable filaments, while the HT Direct leads to shorter and more consistent ones.

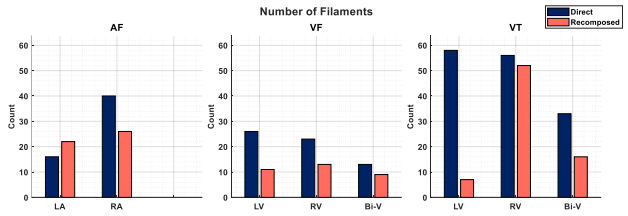

Figure 6. Number of filaments detected for AF, VF, and VT across the optical field, comparing HT Direct and SR phase maps.

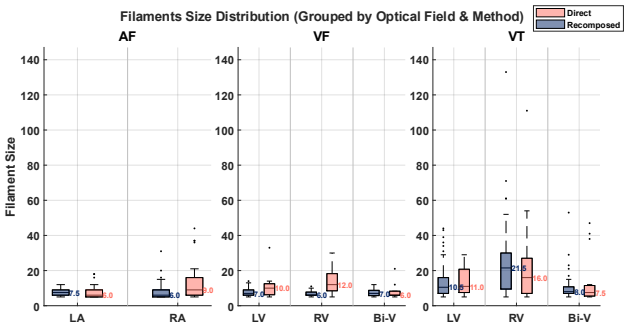

Figure 7. Distribution of filament sizes for AF, VF, and VT across the optical field, comparing HT Direct and SR phase maps.

4. Conclusion

This study evaluated the application of the SR method to reconstruct the instantaneous phase of cardiac optical signals under AF, VT, and VF conditions. Both SR and the HT Direct produced similar phase maps overall, but important differences were observed in the results. SR generated more defined and segmented maps, suggesting better preservation of phase contours, whereas the HT Direct produced smoother maps that favored SPs and filaments identification.

Window selection and noise were shown to influence recomposition and SP detection, and the performance of SR depended strongly on accurate cycle length estimation. Quantitatively, the HT Direct method consistently detected higher numbers of SPs, clusters, and filaments, which may reflect overestimation or unstable patterns. In contrast, SR reduced these detections and may act as a filtering step, favoring longer but more variable filaments.

Overall, SR emerges as a promising alternative to the traditional HT Direct approach, particularly for analyzing reentry patterns in noisy signals or those with non-sinusoidal morphology. As next steps, we plan to extend this analysis to electrical signals to further validate its applicability across different modalities.

Acknowledgments

This work was supported by FAPESP grant #2018/25606-2 and INCT-CNPq INTERAS. The authors acknowledge the use of generative AI tools for language support during the preparation of this manuscript. Specifically, ChatGPT (GPT-4, OpenAI) was used for English translation and refinement, DeepL for translation validation, and Grammarly for grammar and style suggestions. All content was critically reviewed and edited by the authors to ensure scientific accuracy and integrity.

References

[1] Srinivasan NT, Schilling RJ. Sudden cardiac death and arrhythmias. Arrhythm Electrophysiol Rev. 2018 Jun;7(2):111–7.

[2] Attin M, Clusin WT. Basic concepts of optical mapping techniques in cardiac electrophysiology. Biol Res Nurs. 2009 Oct;11(2):195–207.

[3] Kuklik P, Zeemering S, Maesen B, Maessen J, Crijns HJ, Verheule S, et al. Reconstruction of instantaneous phase of unipolar atrial contact electrogram using a concept of sinusoidal recomposition and Hilbert transform. IEEE Trans Biomed Eng. 2015 Jan;62(1):296–302.

[4] Siles, J., Silva, V., Neves, T., Sandoval, I., Quadros, A., Weber, G., Barquero, Ó., Uzelac, I. and Salinet, J. (2025), An integrated platform for 2-D and 3-D optical and electrical mapping of arrhythmias in Langendorff-perfused rabbit hearts. J Physiol. https://doi.org/10.1113/JP287815

Giovanni Viriato Critelli
HeartLab - Biomedical Engineering - CECS
Federal University of ABC - UFABC
Street: Av.Anchieta, São Bernardo do Campo - SP, Brazil
E-mail address: viriato.critelli@aluno.ufabc.edu.br